

Facetted growth of Fe₃Si shells around GaAs nanowires on Si(111)

B. Jenichen,* M. Hilse, J. Herfort, and A. Trampert

Paul-Drude-Institut für Festkörperelektronik,

Hausvogteiplatz 5–7, D-10117 Berlin, Germany

(Dated: May 15, 2022)

Abstract

GaAs nanowires and GaAs/Fe₃Si core/shell nanowire structures were grown by molecular-beam epitaxy on oxidized Si(111) substrates and characterized by transmission electron microscopy. The surfaces of the original GaAs NWs are completely covered by magnetic Fe₃Si exhibiting an enhanced surface roughness compared to the bare GaAs NWs, due to formation of nanofacets. Growth of the shells at the substrate temperature of $T_S = 200$ °C leads to a regular nanofacetted growth of the Fe₃Si shell. The resulting facets of the shells were analyzed, which lead to thickness inhomogeneities of the shells. They consist mainly of well pronounced Fe₃Si(111) planes. The crystallographic orientations of core and shell coincide. The nanofacetted Fe₃Si shells found in the present work are probably the result of the Vollmer-Weber growth mode of Fe₃Si on the {110} side facets of the GaAs NWs.

* bernd.jenichen@pdi-berlin.de

I. INTRODUCTION

Nanowires that combine a semiconductor and a ferromagnet in a core/shell geometry have gained a lot of interest in recent years. [1–6] Because of the cylindrical shape of the ferromagnet, such core/shell nanowires could allow for a magnetization along the wire and thus perpendicular to the substrate surface. Ferromagnetic stripes or tubes with a magnetization perpendicular to the substrate surface have the potential for circular polarized light emitting diodes that optically can transmit spin information in zero external magnetic field and thus allow for on-chip optical communication.[7] They could enable three-dimensional magnetic recording with unsurpassed data storage capacities as well.[8, 9] The combination of the binary Heusler alloy Fe_3Si (Curie temperature of about 840 K) and GaAs has several advantages compared to most of the previously studied semiconductor/ferromagnet (SC/FM) core/shell NWs. The perfect lattice matching and its interface allows for the molecular beam epitaxy (MBE) growth of high quality planar hybrid structures.[10–13] In addition, the cubic Fe_3Si phase, shows a robust stability against stoichiometric variations with only slightly modified magnetic properties.[14] Moreover, its thermal stability against chemical reactions at the SC/FM interface is considerably higher than that of conventional ferromagnets like Fe, Co, Ni, and $\text{Fe}_x\text{Co}_{1-x}$. [10] Recently, we have demonstrated for the first time that GaAs/ Fe_3Si core/shell NWs prepared by MBE show ferromagnetic properties with a magnetization oriented along the NW axis (perpendicular to the substrate surface).[15] However, the structural properties and hence the magnetic properties of the core/shell NWs depend strongly on the substrate temperature during the growth of the Fe_3Si shell.[15, 16] In particular nanofacetting was observed.[16] In this work, we have chosen the sample with most regular facet growth of the Fe_3Si shells around the GaAs(111) oriented cores and analyze the nanofacets by scanning electron microscopy (SEM), transmission electron microscopy (TEM) and selected area diffraction (SAD) in the TEM.

II. EXPERIMENT

GaAs/ Fe_3Si core/shell NW structures are grown by MBE on Si(111) substrates. First, GaAs nanowires are fabricated by the Ga-assisted growth mode on the Si(111) substrates covered with a thin native Si-oxide layer. The growth mechanism is the vapor-liquid-solid

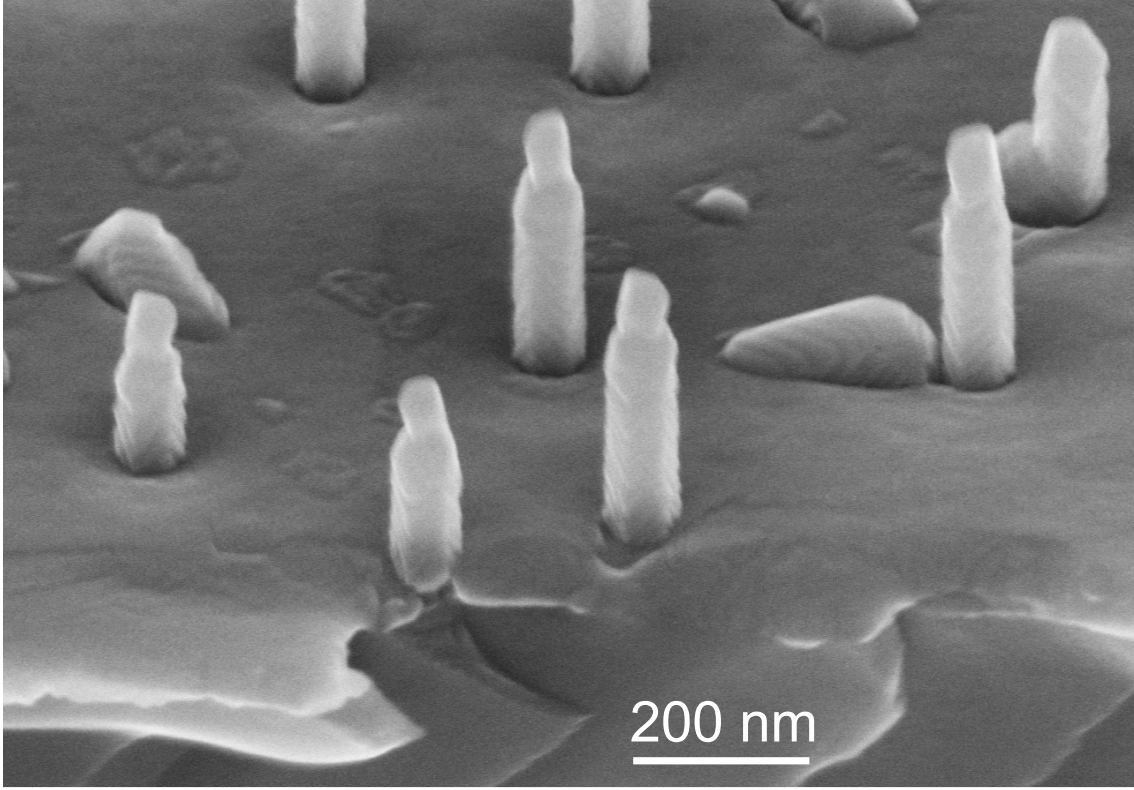


Figure 1. SEM image of GaAs/Fe₃Si core/shell NWs and islands between the NWs grown by molecular beam epitaxy on a Si(111) substrate.

(VLS) mechanism,[17–21] where pin holes in the SiO₂ serve as nucleation sites.[22] A Ga droplet is the preferred site for deposition from the vapor. The GaAs NW then starts to grow by preferential nucleation at the spatially restricted GaAs/Si interface (IF). Further growth is unidirectional and proceeds at the solid/liquid IF. The GaAs NWs are grown at a substrate temperature of 580 °C, and a V/III flux ratio of unity. The equivalent two-dimensional growth rate amounts to 100 nm/h. Once the GaAs NW templates are grown, they are transferred under ultra high vacuum conditions to an As free growth chamber for deposition of the ferromagnetic films. There the GaAs NW templates are covered with Fe₃Si shells at substrate temperatures varying between 100 °C and 350 °C. The NW shells grown at a temperature of 200 °C show a regular nanofacet structure. That is why we perform a careful analysis of the nanofacets using these samples. More details regarding the growth conditions can be found in Ref. [15].

The resulting core/shell NW structures are characterized by SEM, TEM, and SAD in the

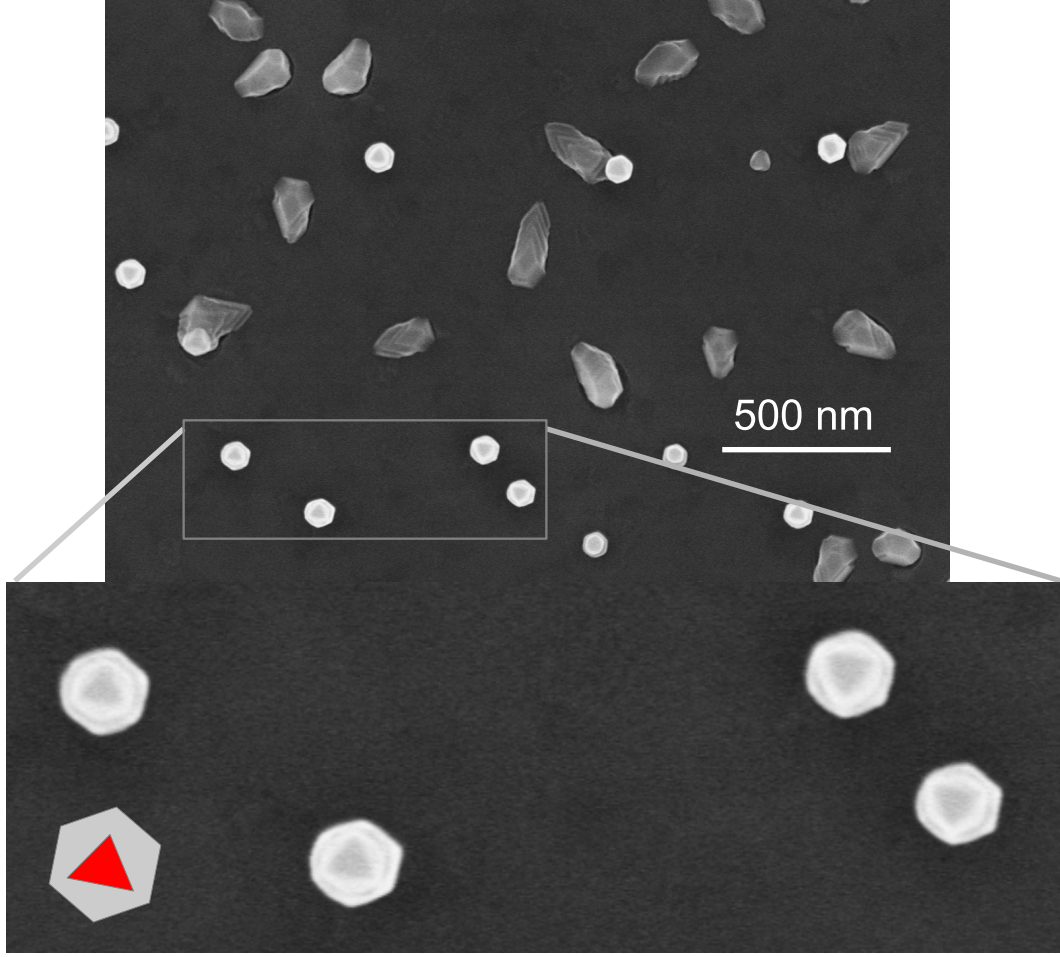


Figure 2. (color online) SEM top view of GaAs/Fe₃Si core/shell NWs and islands between the NWs grown by molecular beam epitaxy on a Si(111) substrate.

TEM. The TEM specimens are prepared by mechanical lapping and polishing, followed by argon ion milling according to standard techniques. TEM images are acquired with a JEOL 3010 microscope operating at 300 kV. The cross-section TEM methods provide high lateral and depth resolutions on the nanometer scale, however they average over the thickness of the thin sample foil or the thickness of the NW as a whole.

III. RESULTS AND DISCUSSION

Figure 1 shows an SEM micrograph of the GaAs/Fe₃Si core/shell NWs. The micrograph of the sample surface reveals a relatively low area density of NWs of about $5 \times 10^8 \text{ cm}^{-2}$. Besides the well oriented NWs we see hillhocks. During the last stage of GaAs NW growth no

more Ga is supplied, and so the remaining Ga in the droplet on top of the NWs is consumed leading to a prolongation of the NW at reduced diameter.[16] The sidewalls of the NWs exhibit regularly nanofaceted surfaces. Figure 2 shows an SEM top view of GaAs/Fe₃Si core/shell NWs grown by MBE on a Si(111) substrate. We observe the typical hexagonal shape of the cross-section of the GaAs/Fe₃Si core/shell NWs (sketched in gray).[16] At higher magnification we observe triangular features (sketched in red) which are connected to the thinner necks of the NWs, where the tilted Fe₃Si(111) planes form extended facets (cf. Fig. 1) intersecting the top Fe₃Si(111) plane, which is parallel to the substrate surface. In this way those characteristic triangles are formed. The lower edges of the necks are more rounded.

Figure 3 demonstrates a multi-beam bright-field TEM micrograph and the corresponding SAD pattern illustrating the orientational relationship of a GaAs/Fe₃Si core/shell NW on Si(111). We observe the coincidence of the core- and shell-orientations, i.e. here the Fe₃Si growth is predominantly epitaxial on the GaAs. In addition the crystallographic orientation of the Fe₃Si shell was checked by high-resolution TEM (not shown here). The straight line drawn on the SAD pattern near the $11\bar{1}$ reflection is oriented perpendicular to the nanofacets of Fe₃Si visible in the corresponding micrograph. The separation of the diffraction spots along this line corresponds to the (111) net plane distance of Fe₃Si indicating that the nanofacets are mainly (111)-oriented. In the SAD pattern from a single core/shell NW the Fe₃Si maxima are stronger probably due to larger volume fraction of the shell. The NWs are approximately 80 nm thick. For the SAD the substrate was first oriented near the [011] zone axis. Then the NW had to be tilted a little further in order to keep the [011] zone axis orientation of the GaAs NW, because the axis of the NW was not exactly perpendicular to the Si surface. In our SAD pattern of the NW the fundamental reflections of the Fe₃Si are more intense than the super-lattice maxima.[11] Nevertheless we can distinguish, $2\bar{2}2$, $3\bar{3}3$, and $4\bar{4}4$ maxima evidencing, that the NW is properly oriented and that the crystallographic orientations of core and shell basically coincide. This underlines that a growth temperature of 200 °C is well suited with respect to reach a highly perfect structure of the Fe₃Si shells. The surface nanofacets are inclined to the (111) net planes parallel to the Si surface by an angle of approximately 118°. The formation of facets reduces the overall surface energy and evidences non negligible material transport over distances small compared to the NW lengths.[23, 24] Unfortunately, the orientation of those surface nanofacets does not coincide

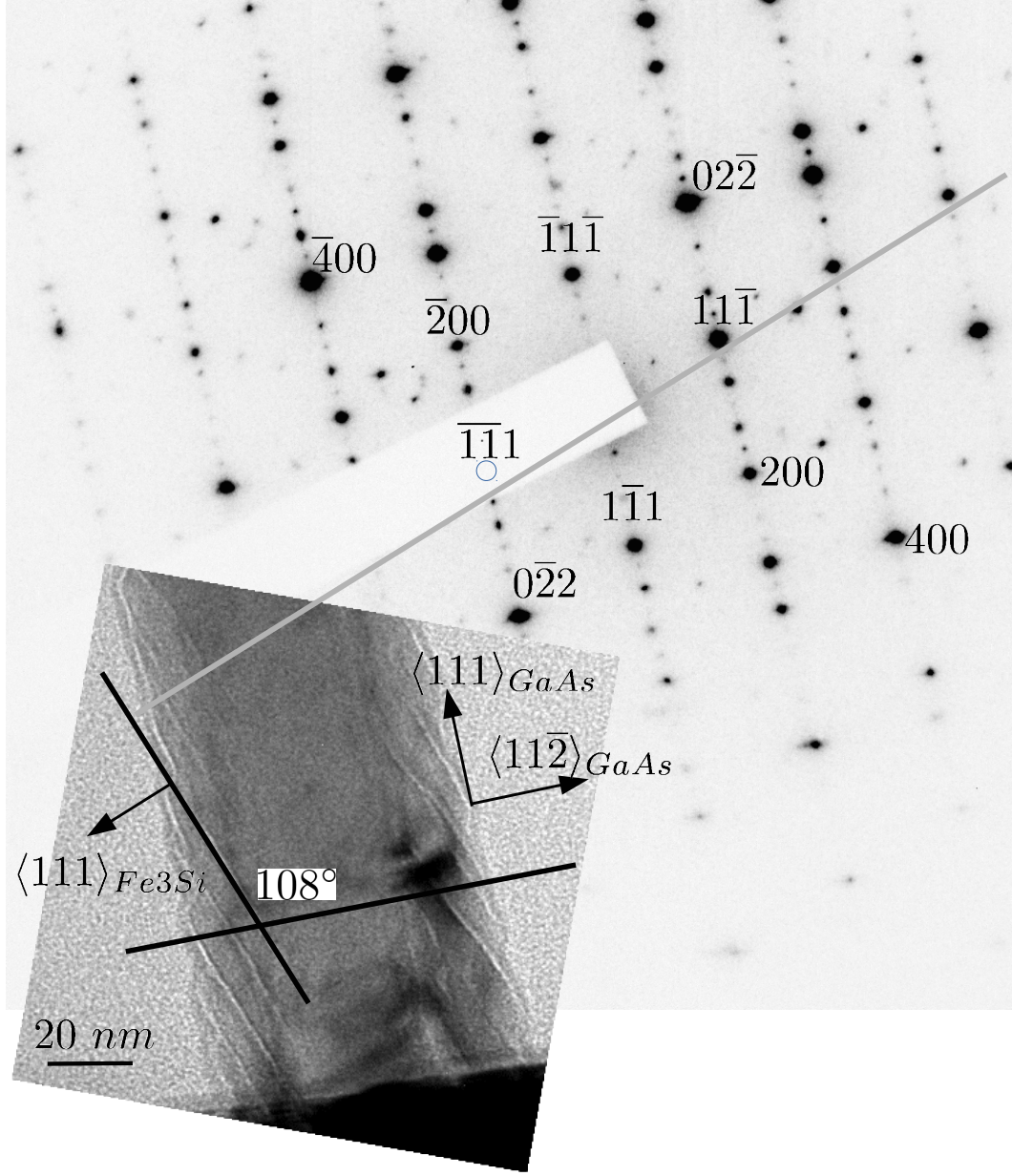


Figure 3. Multi-beam bright-field TEM micrograph and the corresponding SAD pattern illustrating the orientational relationship of a GaAs/Fe₃Si core/shell NW. The straight line near the $11\bar{1}$ reflection is oriented perpendicular to the nanofacets of Fe₃Si visible in the corresponding micrograph.

with those of the facets of the original GaAs NWs corresponding to the $\{110\}$ planes.[25] That is why shell thickness inhomogeneity is caused by faceted growth. On a larger length-scale the Fe₃Si shell is approximately reproducing the shape of the GaAs core NWs.[16]

Layer-by-layer growth could in principle solve the problem of nanofacetting. However,

even planar Fe_3Si grows on GaAs(001) in the Vollmer-Weber (VW) growth mode.[26] Poor wetting during the growth of Fe_3Si on the GaAs surface leads initially to isolated islands, although both lattices match perfectly. We speculate that nanofaceted Fe_3Si shells found in the present work are a result of VW growth mode. In general, one way to improve the homogeneity and the other structural properties of the Fe_3Si -shells could be the use of surfactants. For the growth on GaAs the surfactant materials like e.g. Sb [27], Bi [28], and Te [29] are under discussion.

IV. CONCLUSIONS

The GaAs core NWs grow epitaxially on the bare Si(111) surface inside holes of the SiO_2 film via the VLS growth mechanism. The surfaces of the original GaAs NWs are completely covered by magnetic Fe_3Si . Continuous magnetic shells are established. Growth of the Fe_3Si shells at the substrate temperature of $T_S = 200^\circ\text{C}$ is fully epitaxial and leads to a regular nanofaceted surface. The (111) planes are most pronounced forming a regular pattern around the GaAs NWs. The facetting found in the present work is probably the result of the VW growth mode of Fe_3Si on GaAs.

V. ACKNOWLEDGEMENT

The authors thank Claudia Herrmann, for her support during the MBE growth, Doreen Steffen for sample preparation, Astrid Pfeiffer for help in the laboratory, Anne-Kathrin Bluhm for the SEM micrographs, Esperanza Luna and Uwe Jahn for valuable support and helpful discussion.

VI. REFERENCES

-
- [1] M. Hilse, Y. Takagaki, J. Herfort, M. Ramsteiner, C. Herrmann, S. Breuer, L. Geelhaar, and H. Riechert, Appl. Phys. Lett. **95**, 133126 (2009).

- [2] A. Rudolph, M. Soda, M. Kiessling, T. Wojtowicz, D. Schuh, W. Wegscheider, J. Zweck, C. Back, and E. Reiger, *Nano Lett.* **9**, 3860 (2009).
- [3] D. Rueffer, R. Huber, and P. Berberich, *Nanoscale* **4**, 4989 (2012).
- [4] N. S. Dellas, J. Liang, B. J. Cooley, N. Samarth, and S. E. Mohn, *Appl. Phys. Lett.* **97**, 072505 (2010).
- [5] K. Tivakornsasithorn, R. E. Pimpinella, V. Nguyen, X. Liu, M. Dobrowolska, and J. K. J. Furdyna, *J. Vac. Sci. Technol. B* **30**, 02115 (2012).
- [6] X. Yu, H. Wang, D. Pan, J. Zhao, J. Misuraca, S. Molnar, and P. Xiong, *Nano Lett.* **13**, 1572 (2013).
- [7] R. Farshchi, M. Ramsteiner, J. Herfort, A. Tahraoui, and H. T. Grahn, *Appl. Phys. Lett.* **98**, 162508 (2011).
- [8] S. S. Parkin, M. Hayashi, and L. Thomas, *Science* **320**, 190 (2008).
- [9] K. S. Ryu, L. Thomas, S. H. Yang, and S. S. Parkin, *Appl. Phys. Exp.* **5**, 093006 (2012).
- [10] J. Herfort, H.-P. Schönherr, and K. H. Ploog, *Appl. Phys. Lett.* **83**, 3912 (2003).
- [11] B. Jenichen, V. M. Kaganer, J. Herfort, D. K. Satapathy, H. P. Schönherr, W. Braun, and K. H. Ploog, *Phys. Rev. B* **72**, 075329 (2005).
- [12] J. Herfort, B. Jenichen, V. Kaganer, A. Trampert, H. P. Schoenherr, and K. Ploog, *Physica E* **32**, 371 (2006).
- [13] J. Herfort, A. Trampert, and K. Ploog, *Int. J. Mater. Res.* **97**, 1026 (2006).
- [14] J. Herfort, H. P. Schoenherr, K. J. Friedland, and K. H. Ploog, *J. Vac. Sci. Technol. B* **22**, 2073 (2004).
- [15] M. Hilse, J. Herfort, B. Jenichen, A. Trampert, M. Hanke, P. Schaaf, L. Geelhaar, and H. Riechert, *Nano Lett.* **13**, 6203 (2013).
- [16] B. Jenichen, M. Hilse, J. Herfort, and A. Trampert, *J. Cryst. Growth*, in press **409**.
- [17] R. S. Wagner and W. S. Ellis, *Appl. Phys. Lett.* **4**, 89 (1964).
- [18] B. Mandl, J. Stangl, T. Martensson, A. Mikkelsen, J. Eriksson, L. S. Karlsson, G. Bauer, L. Samuelson, and W. Seifert., *Nano Lett.* **6**, 1817 (2006).
- [19] F. Glas, J. C. Harmand, and G. Patriarche, *Phys. Rev. Lett.* **99**, 146101 (2007).
- [20] A. Fontcuberta, C. Colombo, G. Abstreiter, J. Arbiol, and J. R. Morante, *Appl. Phys. Lett.* **92**, 063112 (2008).

- [21] B. A. Wacaser, K. A. Dick, J. Johansson, M. T. Borgstroem, K. Deppert, and L. Samuelson, *Advanced Materials* **21**, 153 (2009).
- [22] S. Breuer, C. Pfueller, T. Flissikowski, O. Brandt, H. T. Grahn, L. Geelhaar, and H. Riechert, *Nano Lett.* **11**, 1276 (2011).
- [23] G. V. Wulff, *Z. Kristallogr.* **34**, 449 (1901).
- [24] eds: G. Dhanaraj, K. Byrappa, V. Prasad, and M. Dudley, “Handbook of crystal growth,” (Springer, Berlin, Heidelberg, 2010) p. 58.
- [25] J. Grandal, M. Wu, X. Kong, M. Hanke, E. Dimakis, L. Geelhaar, H. Riechert, and A. Trampert, *Appl. Phys. Lett.* **105**, 121602 (2014).
- [26] V. M. Kaganer, B. Jenichen, R. Shayduk, W. Braun, and H. Riechert, *Phys. Rev. Lett.* **102**, 016103 (2009).
- [27] T. Kageyama, T. Miyamoto, M. Ohta, T. Matsuura, Y. Matsui, T. Furuhata, and F. Koyama, *J. Appl. Phys.* **96**, 44 (2004).
- [28] S. Tixier, M. Adamcyk, E. Youngb, J. Schmid, and T. Tiedje, *J. Cryst. Gr.* **251**, 449 (2003).
- [29] N. Grandjean, J. Massies, and V. H. Etgens, *Phys. Rev. Lett.* **69**, 796 (1992).